Supplement of The Cryosphere, 15, 3021–3033, 2021
https://doi.org/10.5194/tc-15-3021-2021-supplement

The Cryosphere Open Access EGU

Supplement of

Three in one: GPS-IR measurements of ground surface elevation changes, soil moisture, and snow depth at a permafrost site in the northeastern Qinghai–Tibet Plateau

Jiahua Zhang et al.

Correspondence to: Tao Che (chetao@lzb.ac.cn)

Supplementary

S1 Monument stability of QLBG

We assess the monument stability of QLBG and its impact on the GPS-IR-measured surface elevation changes and soil moisture content during DOY 182–243 in 2018. We note in section 2 of the main text that the foundation depth of QLBG is slightly shallower than the permafrost table. The monument might settle when the soil around the foundation thaws in late summer. We can obtain the vertical monument movement from the positioning observations of QLBG to examine the monument stability and the necessity of correcting the GPS-IR measurements.

We compute the QLBG's positioning measurements during DOY 182–243 in 2018 in the local NEU (north, east, and up) coordinate reference system, by using GAMIT/GLOBK (http://geoweb.mit.edu/gg/links.php) and four International GNSS Service reference stations BJFS (39.61°N, 115.89°E), JFNG (86.54°N, 114.49°E), URUM (43.81°N, 87.60°E), and LHAZ (29.66°N, 91.10°E). We show the positioning results in Fig. S1.

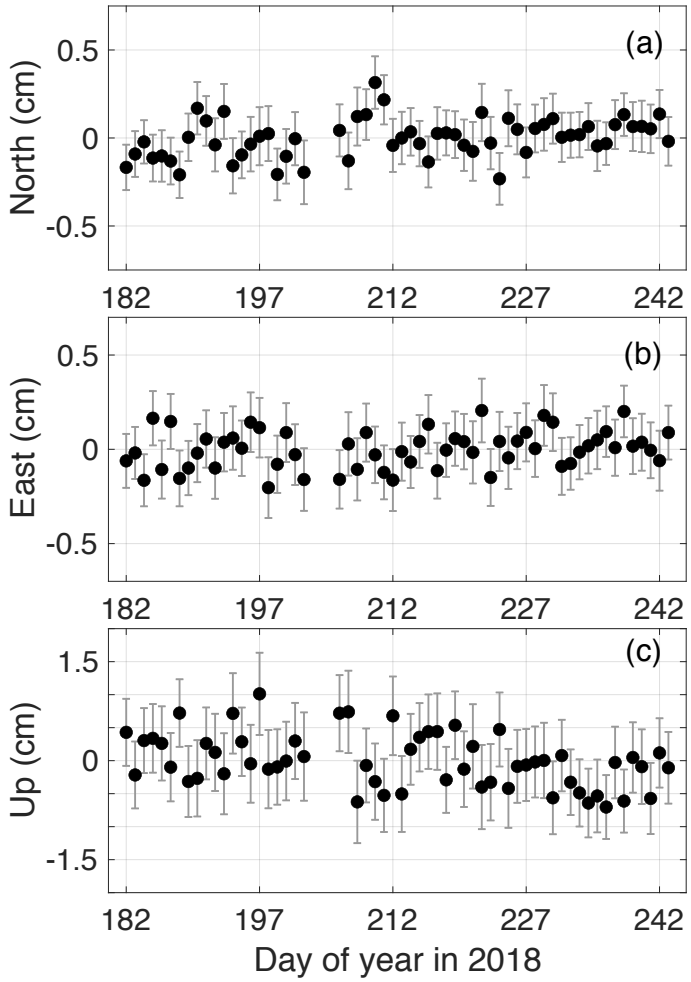

Figure S1: Positioning observations of QLBG in the (a) north, (b) east, and (c) up directions during DOY 182–243 in 2018. They are referenced to their mean values individually.

For the positionings in the east and north directions, their variations are as small as in the range of less than 1 cm. It implies that the monument has no significant inclination and the antenna is still in up-right direction. The positionings in the up direction are composed of the monument displacements and solid earth movement, such as crustal motion and surface deformation due to atmospheric and hydrological surface loadings. Regarding the crustal movement, the velocity field of the contemporary crustal motion of the QTP relative to the Eurasian plate has been constructed (Gan et al., 2007; Liang et al., 2013). The magnitude of the uplift rate of our study site is less than 1 mm/year. The vertical crustal movement during DOY

182–243 in 2018 was negligible. We use the simulations of surface deformation provided by ESMGFZ (Earth System Modelling group of GFZ, Dill and Dobslaw, 2013) to examine the influence of the surface loadings. The simulated values are shown in Fig. S2. During DOY 182–243 in 2018, the variation range of the surface deformation due to atmospheric loading was around 9 mm, and that of continental hydrology was 4 mm. We remove the contributions of the surface loadings from the positionings and use the residuals as the vertical monument movement, which are shown in Fig. S3. The monument movement is relatively noisy, and varies in a range with a magnitude of 1.5 cm. We build a best linear fit for them and find that they do not present a statistically significant trend (The slope of the linear fit line is 0.003 ± 0.004 cm/day, which is not statistically significant (α = 0.05)). We also find that the movement follows a Gaussian normal distribution with a mean of 0 cm and a standard deviation of 0.42 cm. The monument movement barely has an impact on the constant H_0. And they have little impact on the GPS-IR-measured surface elevation changes, as we focus on the temporal variation of the surface elevation.

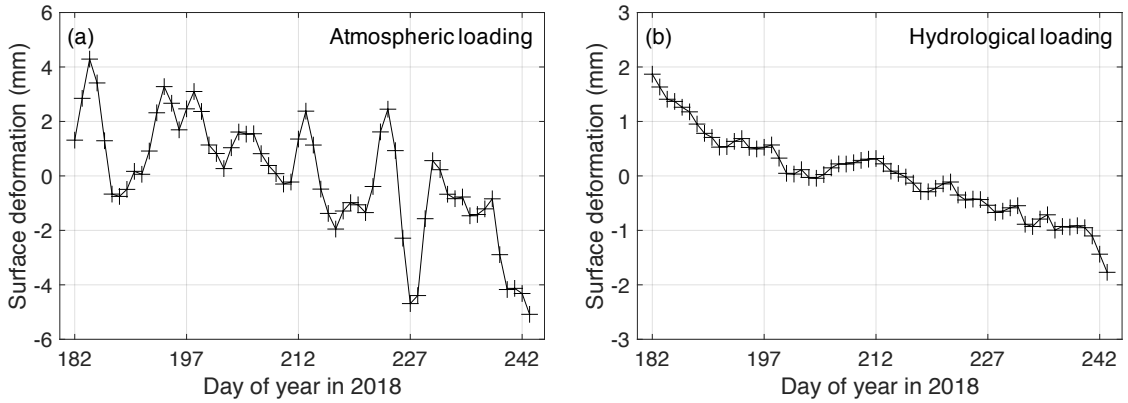

Figure S2: Surface deformation due to (a) atmosphere and (b) continental hydrology, respectively, during DOY 182–243 in 2018. They are referenced to their mean values individually.

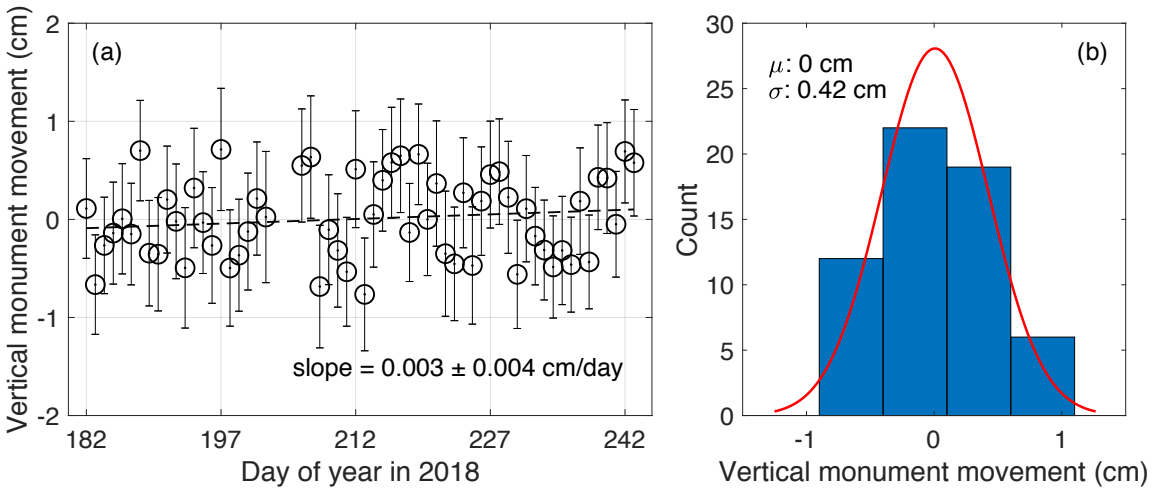

Figure S3: (a) Time series of the vertical monument movement during DOY 182–243 in 2018. Their best linear fit line is also presented (as a dashed line) with the slope of 0.003 ± 0.004 cm/day. (b) Histogram of the vertical monument movement shown in (a) and their normal distribution fit (red curve). The mean (μ) and standard deviation (σ) of this normal fit are 0 cm and 0.42 cm, respectively.

In the modified method, the time-varying $H_0{}'$ is composed of the constant H_0 and the modeled surface elevation changes. Here, we assess the impact of the vertical monument movement on the modeled surface elevation changes through affecting model parameters. When considering the vertical movement (denoted as v hereafter), based on equation (5), the model expression is changed to

$$d(t) + v(t) = d_s \widetilde{I_T} + d_0 \,, \tag{S1}$$

Studying the impact of v on the model parameters is essential to investigate the dependence of v on $\widetilde{I_T}$. We build a scatter plot between v and $\widetilde{I_T}$, which is shown in Fig. S4. The correlation coefficient between them is as weak as 0.14. This result can be expected as the vertical movement is almost white noise whereas the thermal indices possess an increasing trend. The weak correlation indicates that the monument movement has little impact on the estimates of d_s and d_0, then the modeled surface elevation changes. Together with the discussion in the last paragraph, the vertical monument movement has little impact on the time-varying reflector height $H_0{}'$, thus barely affect the phases and soil moisture estimates by our method.

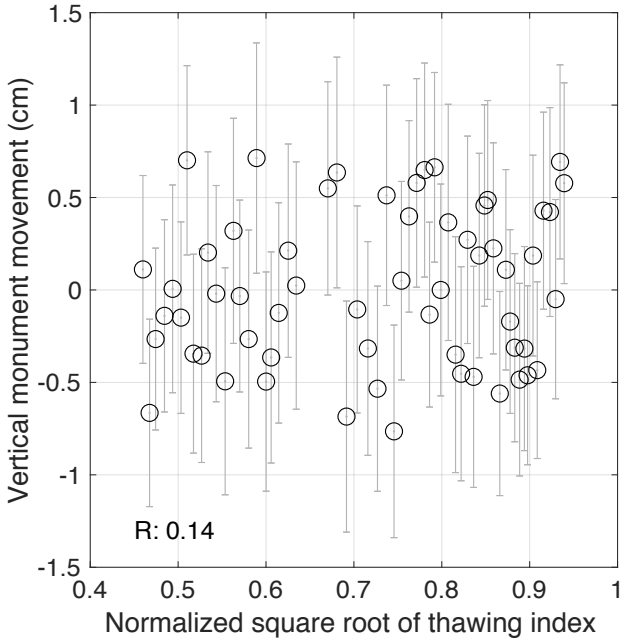

Figure S4: Scatter plot between the square root of normalized thawing index and the vertical monument movement *v* during DOY 182–243 in 2018.

60

S2 Surface reflectivity's impact on GPS-IR-estimated snow depth

To measure snow depth, the reflector height at the beginning of thawing season (H_{ground}) is used as the reference (Fig. S5). Snow depth is derived as the difference between the reflector height of snow surface (H_{snow}) and H_{ground}. Based on the in situ measurements, the mean surface soil moisture at the depth of 1 cm during DOY 167–173 in 2017 was around 38% volumetrically. Given the significant contrast of moisture content between snow and thawed soil, their difference in surface reflectivity for GPS signals might affect the GPS-IR-estimated snow depth.

65

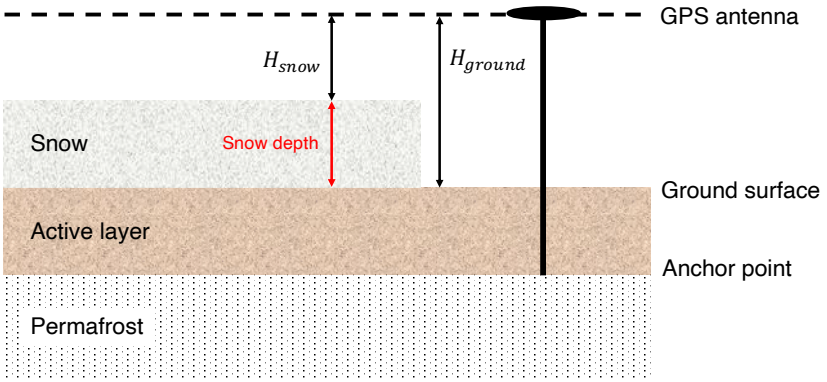

Figure S5: Schematic diagram showing the reflector heights in snow and snow-free conditions, denoted by H_{snow} and H_{ground}. Snow depth is the difference between H_{snow} and H_{ground} serving as a reference. In this study, H_{ground} refers to the average reflector height at the beginning of the thawing season, i.e., DOY 167–173 in 2017.

We use the multipath simulator of Nievinski and Larson (2014) to simulate SNR in the conditions of snow and wet soil. The key parameters for the simulations are presented in Table S1. The simulated SNR observations and their Lomb-Scargle periodogram analysis results are presented in Fig. S6. The dominant reflector height corresponding to the peak power is 1.99 m for snow, whereas 2.03 m for wet soil. The reflectivity difference between snow and wet soil does affect SNR observations and introduces a bias to reflector height retrievals consequently to snow depth measurements. In the simulations, a bias of 4 cm is introduced, which means the GPS-IR measurements overestimate the snow depth.

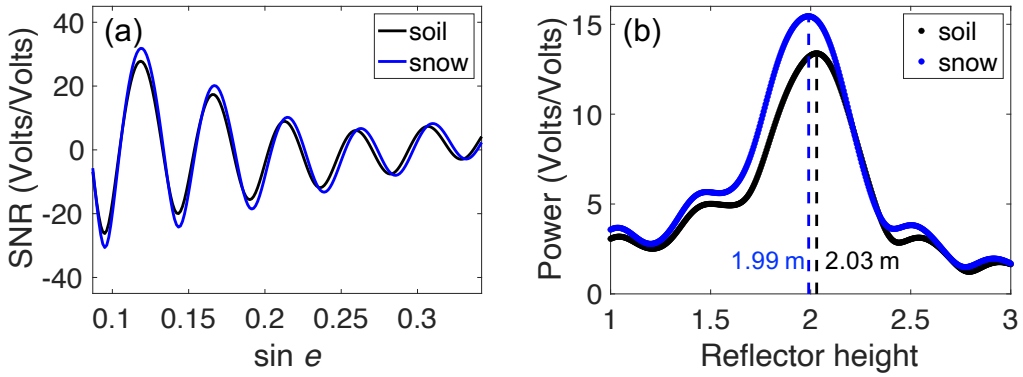

Figure S6: (a) Simulated SNR observations with the reflector of wet soil (black curve) and snow (blue curve). (b) Frequency spectrums of the simulated SNR observations. The frequency has been converted into reflector height. The dominant reflector height corresponding to the peak power is 2.03 m for wet soil, whereas 1.99 m for snow.

Table S1: Key parameters used in the simulations

Parameter	Value
Antenna (Radome)	TRM29659.00 (SCIT)
Signal	L1 C/A
Antenna height	2 m
Azimuth range	90–135°
Elevation angle	5–20°
Snow-free condition	Sandy loam with volumetric moisture content of 38%
Snow-cover condition	Dry snow with default properties in Nievinski and Larson (2014)

References

Dill, R. and Dobslaw, H.: Numerical simulations of global-scale high-resolution hydrological crustal deformations, J. Geophys. Res. Solid Earth, 118(9), 5008–5017, doi:10.1002/jgrb.50353, 2013.

Gan, W., Zhang, P., Shen, Z.-K., Niu, Z., Wang, M., Wan, Y., Zhou, D. and Cheng, J.: Present-day crustal motion within the Tibetan Plateau inferred from GPS measurements, J. Geophys. Res., 112(B8), B08416, doi:10.1029/2005JB004120, 2007.

Liang, S., Gan, W., Shen, C., Xiao, G., Liu, J., Chen, W., Ding, X. and Zhou, D.: Three-dimensional velocity field of present-day crustal motion of the Tibetan Plateau derived from GPS measurements, J. Geophys. Res. Solid Earth, 118(10), 5722–5732, doi:10.1002/2013JB010503, 2013.

Nievinski, F. G. and Larson, K. M.: Forward modeling of GPS multipath for near-surface reflectometry and positioning applications, GPS Solut., 18(2), 309–322, doi:10.1007/s10291-013-0331-y, 2014.